

UCLA

UCLA Previously Published Works

Title

In vitro atherosclerotic plaque and calcium quantitation by intravascular ultrasound and electron-beam computed tomography

Permalink

<https://escholarship.org/uc/item/2wt6g04s>

Journal

American Heart Journal, 131(5)

ISSN

0002-8703

Authors

Gutfinger, Dan E
Leung, Cyril Y
Hiro, Takafumi
[et al.](#)

Publication Date

1996-05-01

DOI

10.1016/s0002-8703(96)90171-4

Copyright Information

This work is made available under the terms of a Creative Commons Attribution License, available at <https://creativecommons.org/licenses/by/4.0/>

Peer reviewed

In vitro atherosclerotic plaque and calcium quantitation by intravascular ultrasound and electron-beam computed tomography

Dan E. Gutfinger, PhD, Cyril Y. Leung, MD, Takafumi Hiro, MD, Bavani Maheswaran, MBBS, Shigeru Nakamura, MD, Robert Detrano, MD, PhD, Xingping Kang, MD, Weiyi Tang, MD, and Jonathan M. Tobis, MD *Irvine and Torrance Calif.*

The purpose of this investigation was to compare the accuracy of intravascular ultrasound (IVUS) and electron-beam computed tomography (EBCT) in quantitating human atherosclerotic plaque and calcium. In experiment I, 12 human atherosclerotic arterial segments were obtained at autopsy and imaged by using IVUS and EBCT. The plaque from each arterial segment was dissected and a volume measurement of the dissected plaque was obtained by water displacement. The plaque from each arterial segment was ashed at 700° F, and the weight of the remaining ashes was used as an estimate of the calcium mass. In experiment II, 11 calcified arterial segments were obtained at autopsy and imaged by using IVUS at one site along the artery. A corresponding histologic cross section stained with Masson's trichrome was prepared. In experiment I, the mean plaque volume measured by water displacement was $165.3 \pm 118.4 \mu\text{l}$. The mean plaque volume calculated by IVUS was $166.1 \pm 114.4 \mu\text{l}$ and correlated closely with that by water displacement ($r = 0.98, p < 0.0001$). The mean calcium mass measured by ashing was $19.4 \pm 15.8 \text{ mg}$. The mean calculated calcium mass by EBCT was $19.9 \pm 17.2 \text{ mg}$ and correlated closely with that by ashing ($r = 0.98, p < 0.0001$). The mean calculated calcium volume by IVUS was $18.6 \pm 11.2 \mu\text{l}$ and correlated linearly with the calcium mass by ashing ($r = 0.87, p < 0.0003$). In experiment II, the mean cross-sectional area of the calcified matrix was $1.71 \pm 0.66 \text{ mm}^2$ by histologic examination compared with $1.44 \pm 0.66 \text{ mm}^2$ by IVUS. There was a good correlation between the calcified cross-sectional area by histologic examination and IVUS ($r = 0.76, p < 0.007$); however, IVUS may underestimate the amount of calcium present depending on the intralésional calcium morphologic characteristics. In conclusion, IVUS accurately quantitates atherosclerotic plaque volume as well as the cross-sectional area and volume of intralésional calcium, especially if the calcium is localized at the base of the plaque. IVUS under-

estimates the amount of calcium present because of signal drop-off when the calcium is too thick for the ultrasound to completely penetrate. In comparison, EBCT accurately quantitates calcium mass regardless of the intralésional calcium morphologic characteristics; however, EBCT does not accurately quantitate plaque volume and will miss noncalcified atherosclerotic lesions. (AM HEART J 1996;131:899-906.)

A method for quantitating atherosclerotic plaque and calcium would be helpful in diagnosing and treating coronary artery disease. Intravascular ultrasound (IVUS) and electron-beam computed tomography (EBCT) are imaging modalities that have been used¹⁻¹⁰ to measure these components of coronary artery disease. IVUS uses high frequency sound waves to produce a reflectance image that has a spatial resolution of 100 μm . It visualizes the components of the arterial wall in cross section and is therefore able to quantitate the extent of plaque that cannot be obtained by angiography. EBCT uses x rays to produce a densitometric image that has a spatial resolution of 500 μm . It is most suitable for visualizing calcium. The primary benefit of EBCT is that it is a noninvasive method that can be used to screen large numbers of patients compared with more invasive methods such as angiography and IVUS.

Previous studies¹⁻³ have shown that EBCT accurately quantitates atherosclerotic calcium mass; however, no studies have shown that EBCT can quantitate noncalcified atherosclerotic plaque. In contrast, comparison studies with histologic examination have shown that IVUS provides an accurate measure of the cross-sectional area (CSA) of noncalcified atherosclerotic plaque,^{4, 5} and there are a few studies that validate IVUS for quantitating atherosclerotic plaque volume.^{6, 7} IVUS can also be used to detect intralésional calcium⁸⁻¹⁰; however, because of "shadowing" and signal dropout caused by calcium,

From the Division of Cardiology, University of California Irvine, and Saint John's Cardiovascular Research Center at Harbor—University of California Los Angeles Medical Center.

Supported in part by NIH grant number RO1HL45077-04A1.

Reprint requests: Jonathan M. Tobis, MD, Division of Cardiology, University of California—Irvine, Bldg. 53, 101 City Drive South, Rt. 81, Orange, CA 92668.

Received for publication Aug. 28, 1995; accepted Oct. 2, 1995.

Copyright © 1996 by Mosby—Year Book, Inc.

0002-8703/96/\$5.00 + 0 4/170750

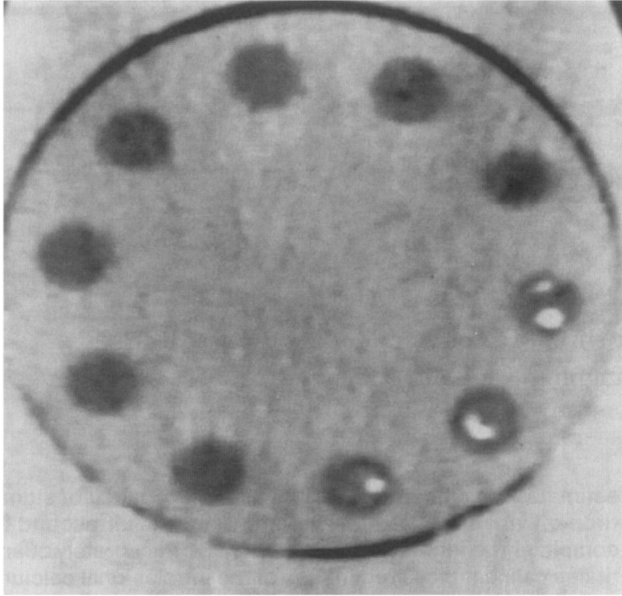


Fig. 1. EBCT image of human arteries inside heart phantom.

reliable quantitation of atherosclerotic calcium by IVUS compared with histologic examination has not been demonstrated. Calcium in IVUS images is commonly quantitated by degrees of arc and lesion length⁸⁻¹⁰; there are no studies evaluating the effectiveness of IVUS in estimating calcium CSA or volume. The objective of this *in vitro* study was to compare the accuracy of IVUS and EBCT in quantitating human atherosclerotic plaque and calcium.

METHODS

Experiment I: Volume and mass measurement of plaque and calcium

Intravascular ultrasound imaging. Twelve human atherosclerotic arterial segments (11 coronary and 1 iliac side branch) were obtained at autopsy from 12 cadavers (8 men and 4 women) ranging in age from 41 to 96 years with a mean age of 62.8 ± 16.9 years. The arteries were stored in normal saline at 4° C and were not fixed in formalin until after IVUS imaging was completed. IVUS imaging was performed within 48 hours after autopsy. For each artery two surgical needles were placed through the adventitia of the artery to provide acoustic reference points for the starting and ending points during a pullback of each arterial segment. The artery was connected to an 8F coronary guiding catheter that was pressurized with normal saline within a closed system to permit imaging under physiologic pressures (100 mm Hg). The artery was immersed in a normal saline bath at room temperature during imaging. A 25-MHz IVUS catheter (InterTherapy/CVIS, Sunnyvale, Calif.) with a motorized pullback device was used to capture serial cross-sectional images of the arterial segment between the two surgical needles on super-VHS videotape at 30 frames/sec with a pullback rate of 0.25 mm/sec. At

completion of IVUS imaging, each of the needle sites was marked with silk suture and the needles were removed. The arteries were then pressure perfused at 100 mm Hg for 24 hours in 10% formalin. Subsequently the arterial segment localized between the two suture marks was excised, and the remaining arterial specimen was discarded. The excised arterial segments ranged in length from 5 mm to 37 mm with a mean length of 17.0 ± 11.3 mm. The arterial segments were stored in formalin at room temperature until EBCT imaging was performed.

EBCT imaging. EBCT imaging was performed by using an electron beam scanner (Imatron, South San Francisco, Calif.). This scanner was calibrated so that a CT number of 0 corresponded to the linear mass attenuation coefficient of pure water. Two scans were performed for each arterial segment. In the first scan, a 30-cm field of view was used, and this was immediately followed by a second scan with a 9-cm field of view to provide increased spatial resolution. Both scans were performed with a 3-mm slice thickness. Each image consisted of $512 \times 512 \times 3$ mm volume elements (voxels). The arterial segments during EBCT imaging were placed inside a chest phantom as previously described.^{2,3} No changes in the chest phantom orientation or position were made between the two scans. This phantom contained regions corresponding to the chest wall, lungs, vertebral column, and heart. The heart region had 10 cylinders arranged in a circle, as illustrated in Fig. 1). Each cylinder was filled with normal saline, and care was taken to eliminate all air bubbles. Arterial segments were placed in only five of the cylinders, located in the right half of the heart region. The remaining five cylinders in the left half of the heart region were filled with only normal saline so that each cylinder containing an arterial segment had a corresponding contralateral cylinder filled with saline. These saline-filled cylinders provided reference CT numbers, which were used to overcome beam hardening effects.¹¹ A standard bone mineral phantom (0, 50, 100, 200 mg/ml calcium hydroxyapatite) developed by Arnold and Rowberg^{12,13} was placed on top of the chest phantom during scanning. This standard bone mineral phantom was visible only in the EBCT images with the 30-cm field of view and provided a correlation between calcium hydroxyapatite density and CT number for each image slice. Because a maximum of only five arterial segments could be imaged during each EBCT scan, six separate scans (three with a 30-cm field of view and three with a 9-cm field of view) were required to image all 12 arterial segments.

Plaque mass and volume measurement. At the completion of EBCT imaging, the arterial segments were removed from the chest phantom. Each arterial segment was "filet-opened" by performing a single longitudinal cut through all layers of the arterial wall along the long axis of the artery. The site for the single longitudinal cut was chosen to be in the region with the least amount of atherosclerotic plaque. The plaque was then separated in its entirety by peeling back the overlying media, adventitia, and perivascular tissue along the natural dissection plane localized between the plaque and media. The dissected plaque, free of media and adventitia, was then weighed, and a volume measure-

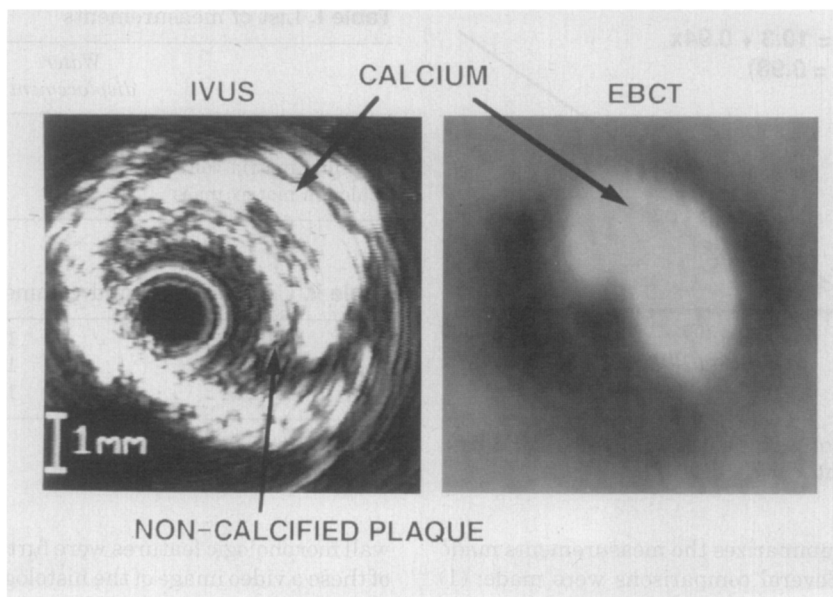


Fig. 2. IVUS image of calcified artery with corresponding EBCT image.

ment was made by water displacement inside a calibrated 1 ml syringe.

Calcium mass measurement. All the tissue for each arterial segment was saved inside a separate glass flask, whose dried emptied weight was determined. Each of the flasks was placed inside an oven at 700° F for 72 hours. The total calcium mass for each arterial segment was then measured as the difference between the weight of the flask containing the remaining ashes and the weight of the dried empty flask.^{3, 14}

IVUS image analysis. The IVUS images were digitized (RasterOps 24 STV board; Mediagrabber software, Santa Clara, Calif.) from the super-VHS videotape at 0.5 mm intervals along the artery length and stored on a computer (Macintosh IICI, Apple, Cupertino, Calif.). The starting and ending points of each arterial segment were identified on the videotape by the presence of the acoustic needles. The pullback rate (0.25 mm/sec) multiplied by the time interval on the videotape between the appearance of the starting and ending acoustic needles was used as an estimate of the arterial segment length. The plaque CSA was then traced in each image by an operator-guided cursor, and a quantitative measurement of the plaque CSA was obtained by an image processing software package (NIH Image, Internet public domain software). The total volume of plaque for each arterial segment was then calculated by summing the individual plaque CSAs over the length of the artery as follows:

$$\text{Volume} = \frac{\text{Length}}{N} \times \sum_{i=1}^{N-1} \left(\frac{\text{CSA}_i + \text{CSA}_{i+1}}{2} \right)$$

where length denotes the arterial segment length, CSA_i denotes the i^{th} CSA, and N denotes the total number of images grabbed for the arterial segment.

In estimating the calcium matrix volume from IVUS, the same procedure was used; but instead of tracing the plaque CSA in each image, the calcium CSA was traced. Two criteria had to be simultaneously satisfied to identify a calcified region. First, the calcified region had to produce a highly echogenic signal that was uniformly saturated in intensity and localized within the region corresponding to the vessel wall. Second, the calcified region had to produce either signal drop-off or some degree of signal attenuation (shadowing) from the tissues peripheral to the calcified region. It was noted that when the ultrasound catheter was advancing through a calcified lesion, there was a gradual increase and decrease in the degree of shadowing and that shadowing was apparent only after the catheter had advanced partly through the calcified lesion. Therefore the second criteria was relaxed if, after reviewing the videotape in real time, it was clear that a highly echogenic region corresponded to the tail end of a calcified lesion. The area traced for each calcified region contained only the highly echogenic region that was uniformly saturated in intensity. No attempt was made to include areas of signal drop-off or shadowing. Fig. 2 illustrates an IVUS image and the corresponding EBCT image.

EBCT image analysis. The EBCT images were processed online by using the computer system associated with the scanner. Each arterial segment was analyzed separately. Within each 9-cm field of view, the region corresponding to the cylinder containing the arterial segment was first analyzed for evidence of calcium. The criterion for identifying a calcified region was the presence of at least one voxel with a CT number >100 Hounsfield units.³ If this criterion was not satisfied, then the contribution of this image slice to the calcium mass was considered to be 0. If there was evidence of calcium, the image slice was further analyzed by a mathematical model that takes into account partial volume effects (see Appendix).^{3, 15}

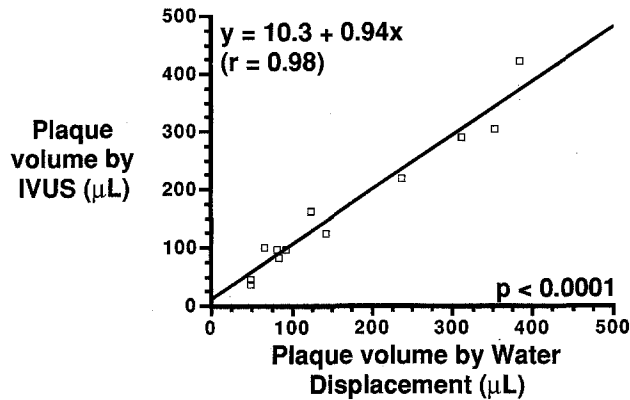


Fig. 3. Correlation between plaque volume by IVUS and by water displacement.

Statistics. Table I summarizes the measurements made in this experiment. Several comparisons were made: (1) plaque volume from intravascular ultrasound was compared with that from water displacement; (2) calcium matrix volume from IVUS was compared with calcium mass from ashing; and (3) calcium mass from EBCT was compared with that from ashing. For each comparison a paired *t* test and linear regression analysis were performed. In addition, the Z-transformation was used to compare the correlation coefficients derived for comparisons (2) and (3). To assess the variability of the CSA measurements made for the calcified regions in the IVUS images, a second blinded independent observer traced the calcium cross section in 123 images. Interobserver variability was assessed by linear regression analysis.

Experiment II: Measurement of calcium CSA

IVUS imaging. Twenty three iliac artery segments were obtained at autopsy from 7 cadavers (2 male and 5 female, aged 15 to 86 years with a mean age of 58 years). Within 3 hours of autopsy, the arteries were pressure perfused for 24 hours in 10% formalin and then stored in formalin at room temperature until IVUS imaging was performed. For each arterial segment, a surgical needle was placed through the adventitia of the artery to provide an acoustic reference point. IVUS imaging was then performed inside a normal saline bath by using a 25-MHz IVUS catheter (InterTherapy/CVIS). IVUS images were acquired on super-VHS video tape at the site where the acoustic needle was detected. At completion of IVUS imaging, the site of the surgical needle was marked with silk suture.

Histologic examination. The arteries were placed inside a decalcification solution (SP Decalcifying Solution, Baxter Scientific, Irvine, Calif.) for 72 hours. The arterial segments were then embedded in paraffin and sectioned at the site that was marked with silk suture. The histologic cross sections were stained with Masson's trichrome.

IVUS analysis. The IVUS images were digitized and analyzed in the same way as in the first experiment.

Histologic analysis. The histologic sections were first reviewed for crush artifacts during microtome sectioning. Only those histologic sections that had preserved vessel

Table I. List of measurements

	Water displacement	IVUS	EBCT	Ashing
Plaque volume	✓	✓		
Calcium matrix volume		✓		
Calcium matrix mass			✓	✓

Table II. Calcium mass and volume

EBCT	19.9 ± 17.2 mg
IVUS	18.6 ± 11.2 µl
Ashing	19.4 ± 15.8 mg

Values are mean ± SD. *p* NS.

wall morphologic features were further analyzed. For each of these a video image of the histologic section was fed from a microscope (Leica, model Wild M3Z, Rockleigh, N.J.) through a video camera (Sony, CCD-IRIS/RGB, model DXC-151A, Tokyo, Japan) into a computer (Macintosh IICI, Apple) and digitized (RasterOps 24STV board; Mediagrabber software). A slide with calibration marks at 0.1 mm was imaged through the microscope and digitized to provide an appropriate magnification scale. The CSA of the decalcified region was then traced with an operator-guided cursor, and a quantitative measurement of the CSA was obtained by the same software program used to analyze the IVUS images.

Statistics. The calcium CSA by IVUS was compared with that by histologic examination by linear regression analysis and a paired *t* test.

RESULTS

Experiment I. IVUS was able to detect plaque in all 12 arterial segments, while EBCT was able to detect calcium in all 11 arterial segments that contained calcium after ashing. There was no evidence of calcium by both EBCT and IVUS in the twelfth arterial segment. Although this arterial segment had 48.6 mg of plaque after dissection, there was no evidence of disease by EBCT because the plaque in this arterial segment consisted of noncalcified atheroma.

The mean plaque volume measured by water displacement from the 12 arterial segments was 165.3 ± 118.4 µl. The mean plaque weight was 167.8 ± 115.0 mg. The mean plaque volume calculated from the ultrasound images was 166.1 ± 114.4 µl. The correlation coefficient between the measurements of plaque volume by water displacement compared with that by the IVUS images was $r = 0.98$ ($p < 0.0001$) (Fig. 3).

The mean calcium mass measured by ashing from the 12 arterial segments was 19.4 ± 15.8 mg. The mean calcium mass calculated from the EBCT im-

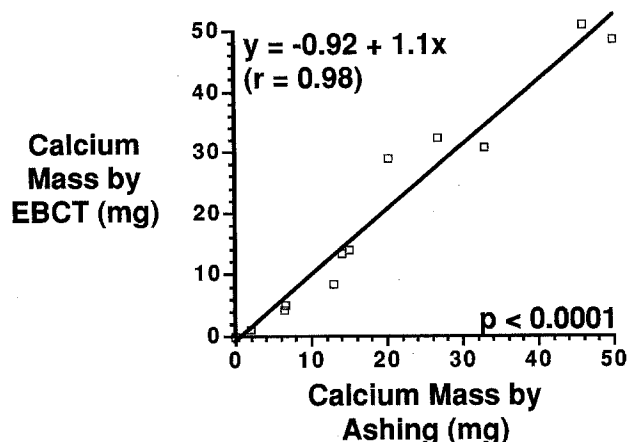


Fig. 4. Correlation between calcium mass by EBCT and by ashing.

Table III. Comparison of correlation coefficients

Linear regression	r Value	p Value
Ashing vs EBCT	0.98*	0.0001
Ashing vs IVUS	0.87*	0.0003
UFCT vs IVUS	0.82	0.0012

* $p < 0.05$

ages was 19.9 ± 17.2 mg. The mean calcium matrix volume calculated from the IVUS images was 18.6 ± 11.2 μ l. Calcium mass and volume are shown in Table II. The correlation coefficients between the calcium mass by ashing compared with EBCT and IVUS are shown in Table III. The correlation between the measurements of calcium mass by EBCT compared with that by ashing ($r = 0.98$) was with statistical significance ($p < 0.05$) greater than the correlation between the measurements of calcium matrix volume by IVUS and the calcium mass by ashing ($r = 0.87$) (Figs. 4 and 5).

Although the correlation between calcium mass by EBCT and that by ashing was excellent ($r = 0.98$, $p < 0.0001$), the correlation between calcium mass by EBCT and the measured dissected plaque mass ($r = 0.67$, $p < 0.02$) was not as close (Fig. 6). Moreover, the mean calcium mass by EBCT (19.9 ± 17.2 mg) was one order of magnitude smaller than the mean measured dissected plaque mass (167.8 ± 115.0 mg).

The mean calcium CSA in 123 IVUS images measured by two independent observers was 1.04 ± 0.92 mm^2 for observer A compared with 1.14 ± 1.00 mm^2 for observer B. The correlation coefficient between the measurements made by observers A and B was $r = 0.98$ ($p < 0.0001$). Observer B had a mean positive

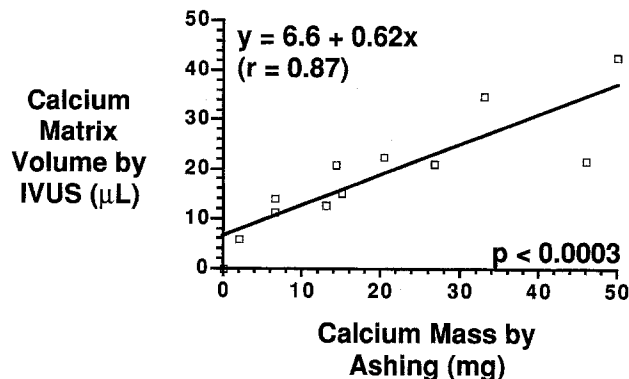


Fig. 5. Correlation between calcium matrix volume by IVUS and calcium mass by ashing.

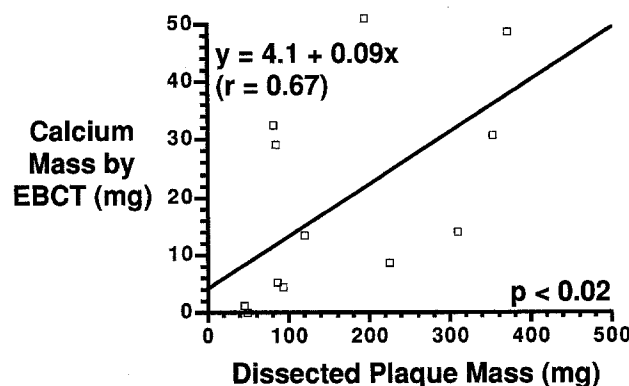


Fig. 6. Correlation between calcium mass by EBCT and measured dissected plaque mass.

bias of 0.1 ± 0.2 mm^2 relative to observer A, which clinically is an acceptable variation.

Experiment II. From the 23 arterial segments processed, only 17 (74%) had evidence of calcified atherosclerosis by histologic examination, but only 11 (48%) had acceptable histologic cross sections in which the vessel wall morphologic features were preserved so that the calcium CSA could be measured. For these 11 histologic cross sections the mean CSA of the calcified region was 1.71 ± 0.66 mm^2 . The mean CSA of the calcified matrix from the 11 corresponding IVUS images was 1.44 ± 0.66 mm^2 . There was not a statistically significant difference between these means by the paired t test. The correlation coefficient between the calcified CSA determined by histologic examination and IVUS was $r = 0.76$ ($p < 0.007$), Fig. 7.

To further explore how IVUS images represent the geometric deposition of calcium within a plaque, the histologic cross sections of the 11 specimens from experiment II were reexamined, and each was classified into one of three types according to the location

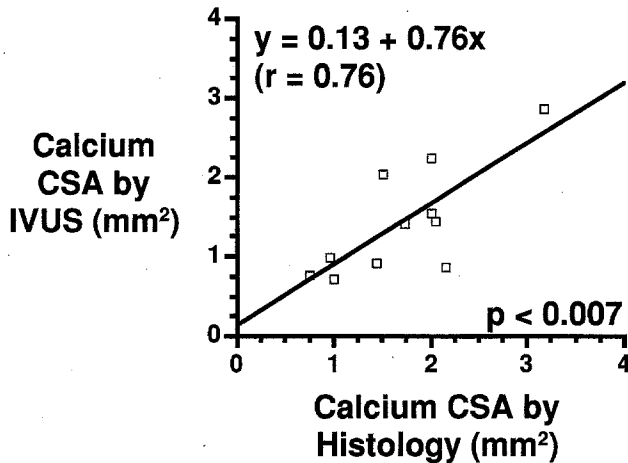


Fig. 7. Correlation between calcium CSA by IVUS and by histologic examination.

of the intralésional calcium within the plaque. Fig. 8 shows a sketch illustrating the three histologic types. Intralésional calcium localized at the base of the plaque was classified as type I. Intralésional calcium localized more superficially within the plaque so that plaque extended behind the calcium was classified as type II. Intralésional calcium that consisted of two separate pieces of calcium with one behind the other was classified as type III. Of the 11 specimens, 7 (64%) were classified as type I, 3 (27%) were classified as type II, and 1 (9%) was classified as type III. Whereas histologic types I and II were accurately represented by IVUS imaging, the deeper calcified area of histologic type III was obscured by shadowing from the more centrally located calcified matrix and led to underestimation of the calcium CSA by IVUS.

DISCUSSION

This *in vitro* study demonstrates that IVUS is valuable in quantitating atherosclerotic plaque and calcium, and EBCT accurately predicts only the amount of calcium present in the plaque. EBCT accomplishes this in a noninvasive manner, and it is therefore useful as a screening test for the presence of coronary artery calcium. IVUS is an invasive procedure but provides an accurate image of the plaque cross-sectional morphologic features, which can otherwise only be obtained by histologic examination. In addition, the estimation of plaque volume by IVUS correlates closely with the actual plaque volume measured by water displacement ($r = 0.98$, $p < 0.0001$).

Since the majority (76%)⁹ of significant lesions have some amount of calcification present, calcium is

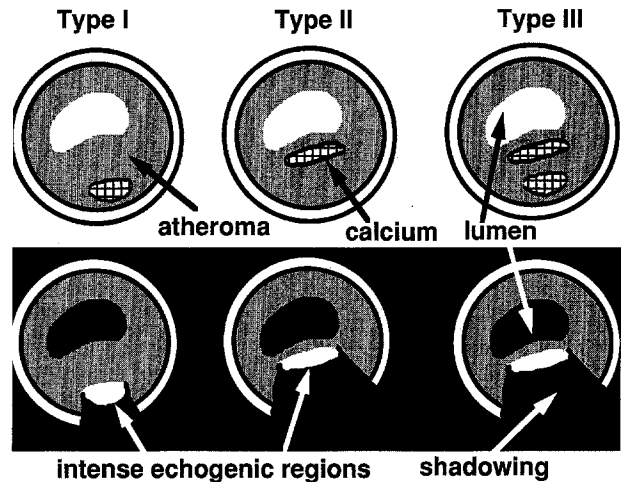


Fig. 8. Intralésional calcium location types. *Top*, Histologic analysis; *bottom*, IVUS.

a good marker for the presence of disease.^{16, 17} In one recent study in particular, the calcium area noted by EBCT could be used to discriminate between patients with and without significant disease with an overall accuracy of 83%.¹⁶ However, if the atherosclerotic plaque is noncalcified, as demonstrated in experiment I, EBCT will not identify such lesions; it is therefore not as accurate as IVUS in quantitating the extent of noncalcified atherosclerosis. One may argue, however, that if none of the lesions are calcified, then the extent of the disease is most likely not severe enough to be clinically significant.^{9, 16, 17} Experiment I also demonstrates that the calcium mass estimated by EBCT correlates with the measured dissected plaque mass ($r = 0.67$, $p < 0.02$); however, the mean calcium mass by EBCT (19.9 ± 17.2 mg) was one order of magnitude smaller than the measured mean dissected plaque mass (167.8 ± 115.0 mg). This suggests that the calcified portion of the plaque is only a small part of the entire atherosclerotic lesion. Nonetheless, because EBCT estimates calcium mass with great accuracy, it may be reliable in serially tracking the progression of calcium in coronary arteries.

In this study it was demonstrated that IVUS is effective in quantitating the CSA and the total volume of the calcified matrix. Although IVUS cannot quantitate total calcium mass directly, a specific density of 1 mg/ μ l may be used to convert the volume measurement to a mass estimate. Our data show that the correlation between calcium volume by IVUS and calcium mass by ashing ($r = 0.87$, $p < 0.0003$) is very close—but statistically less close than the correlation between calcium mass by EBCT and that by ashing ($r = 0.98$, $p < 0.0001$).

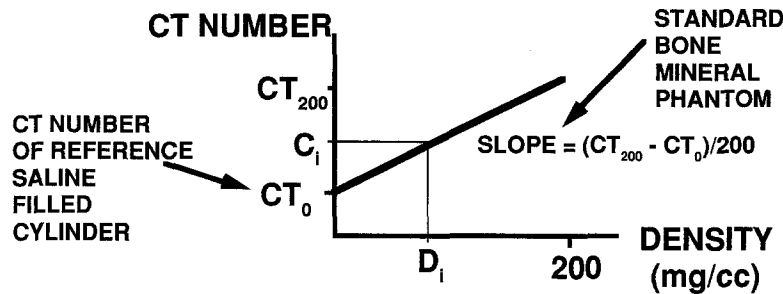


Fig. 9. Calcium density estimation.

The ability of IVUS to quantitate calcium CSA or volume has previously been questioned because of the shadowing effect produced by calcium. It was therefore expected that IVUS would tend to underestimate the amount of calcium; however, no statistically significant underestimation was demonstrated in either experiment. The accuracy of IVUS in quantitating the calcium CSA depends on the intralésional calcium location (Fig. 8). Shadowing is less likely to interfere with calcium CSA measurement when the calcium is localized at the base of the plaque (type I histologic pattern) because the thickness of the calcium is narrow and there is no component of the calcium that is shadowed. For intralésional calcium that is more superficially localized (type II histologic pattern), it is unclear how accurate IVUS is in quantitating the calcium CSA because the depth of IVUS penetration into the calcified lesion is limited. Thus it is likely that for thick type II lesions IVUS may penetrate only partially and therefore lead to underestimation of calcium. For intralésional calcium that consists of two separate pieces of calcium with one behind the other (type III histologic pattern), the more peripheral piece of calcium is likely to be shadowed and will also lead to underestimation of calcium by IVUS.

Study limitations. The analysis of the histologic cross sections of experiment II shows the presence of different types of intralésional calcium location. Since only 11 specimens were used, the prevalence of these histologic types is unknown. Type III represents the most challenging morphologic feature for accurate calcium quantitation by IVUS. In experiment I, no histologic pattern was used to validate the plaque and calcium volume measurements because the arteries were sacrificed during ashing. It is unclear what percentage of the 12 specimens from experiment I had calcium with type III histologic pattern. If none of the 12 specimens had calcium with type III histologic pattern, the results would be biased toward a good correlation with ashing.

The criterion for identifying a calcified region in

the EBCT images is based on a single-voxel threshold.³ This criterion was satisfactory in our in vitro setting in which measurements of calcium were restricted only to the cylindrical regions. In an in vivo setting, where motion artifacts are present and the exact location of arteries is not known in advance, using a single voxel to define a calcified region may lead to error.¹⁸ We therefore agree that by using a series of contiguous voxels¹⁸ with CT numbers greater than a specified threshold would be a more suitable criterion.

Conclusion. IVUS can accurately quantitate atherosclerotic plaque volume and is also useful in quantitating the CSA and volume of intralésional calcium. However, IVUS may underestimate the amount of calcium present depending on the intralésional calcium morphologic features. For intralésional calcium localized at the base of the plaque, or for more superficial calcium that is thin, IVUS accurately quantitates the amount of calcium present. In comparison, EBCT accurately quantitates calcium mass regardless of the intralésional calcium morphologic features. EBCT however, cannot be used to accurately quantitate atherosclerotic plaque mass and will miss noncalcified atherosclerotic lesions.

We thank Kris Ekberg and Nathan D. Wong, PhD. Specimens for this study were provided by the Orange County Coroner's Office, James Beisner, Chief Deputy Coroner.

REFERENCES

1. Agatston AS, Janowitz WR, Hildner FJ, Zusmer NR, Viamonte M, Detrano R. Quantification of coronary artery calcium using ultrafast computed tomography. *J Am Coll Cardiol* 1990;50:827-32.
2. Mahaisavariya P, Detrano R, Kang X, Garner D, Vo A, Georgiou D, Molloy S, Brundage BH. Quantitation of in-vitro coronary artery calcium using ultrafast computed tomography. *Cathet Cardiovasc Diag* 1994;32:387-93.
3. Detrano R, Weihi T, Kang X, Mahaisavariya P, McCrae M, Garner D, Peng SK, Measham C, Molloy S, Gutfinger D, Nickerson S, Brundage B. Accurate coronary calcium phosphate mass measurements from electron beam computed tomograms. *Am J Card Imaging* 1995;9:167-73.
4. Gussenhoven WJ, Essed CE, Frietman P, Mastik F, Lancee C, Slager C, Serruys P, Gerritsen P, Pieterman H, Bom N. Intravascular

echogenic assessment of vessel wall characteristics: a correlation with histology. *Int J Card Imaging* 1989;4:105-16.

5. Nishimura RA, Edwards WD, Warnes CA, Reeder GS, Holmes DR, Tajik AJ, Yock PG. Intravascular ultrasound imaging: in vitro validation and pathologic correlation. *J Am Coll Cardiol* 1990;16:145-54.
6. Cavaye DM, White RA, Kopchok GE, Mueller MP, Maselly MJ, Tabbara MR. Three-dimensional intravascular ultrasound imaging of normal and diseased canine and human arteries. *J Vasc Surg* 1992;16:509-19.
7. Coy KM, Park JC, Fishbein MC, Laas T, Diamond GA, Adler L, Maurer G, Siegel RJ. In vitro validation of three-dimensional intravascular ultrasound for the evaluation of arterial injury after balloon angioplasty. *J Am Coll Cardiol* 1992;20:692-700.
8. Fitzgerald PJ, Portis TA, Yock PG. Contribution of localized calcium deposits to dissection after angioplasty: an observational study using intravascular ultrasound. *Circulation* 1992;80:64-70.
9. Mintz GS, Douek P, Pichard AD, Kent KM, Satler LF, Popma JJ, Leon MB. Target lesion calcification in coronary artery disease: an intravascular ultrasound study. *J Am Coll Cardiol* 1992;20:1149-55.
10. Friedrich GJ, Moes NY, Muhlberger VA, Gabl C, Mikuz G, Hausmann D, Fitzgerald PJ, Yock PG. Detection of intraluminal calcium by intracoronary ultrasound depends on the histologic pattern. *AM HEART J* 1994;128:435-41.
11. Zerhouni E, Spivey J, Morgan R, Leo F, Stitik F, Siegelman S. Factors influencing quantitative computed tomographic measurements of solitary pulmonary nodules. *J Comput Assist Tomogr* 1982;6:1075-87.
12. Arnold BA, Rowberg AH. QCT of lung nodules with a simultaneously scanned bone mineral phantom and automated software. Presented at RSNA, Chicago, November 1988.
13. Arnold BA, Rowberg AH. Automated image detail localization method. United States patent number 4922915. May 8, 1990.
14. Molloy S, Detrano R, Ersahin A, Roeck W, Morcos C. Quantification of coronary arterial calcium by dual energy digital subtraction fluoroscopy. *Medical Physics* 1991;18:295-98.
15. Gutfinger D, Hertzberg E, Tolxdroff T, Greensite F, Sklansky J. Tissue identification in MR images by adaptive cluster analysis. Proceedings of SPIE Medical Imaging V: Imaging Processing, 1445, San Jose, California, March 1991, pp. 288-96.
16. Kaufmann RB, Peyser PA, Sheedy PF, Rumberger JA, Schwartz RS. Quantification of coronary artery calcium by electron beam computed tomography for determination of severity of angiographic coronary artery disease in younger patients. *J Am Coll Cardiol* 1995;25(3):626-32.
17. Rumberger JA, Schwartz RS, Simons DB, Sheedy PF 3rd, Edwards WD, Fitzpatrick LA. Relation of coronary calcium determined by electron beam computed tomography and lumen narrowing determined by autopsy. *Am J Cardiol* 1994;73(16):1169-73.
18. Kaufmann RB, Sheedy PF, Breen JF, et al: Detection of heart calcification with electron beam CT: interobserver and intraobserver reliability for scoring quantification. *Radiology* 1994;190:347-52.

APPENDIX

To calculate the calcium mass from the EBCT images, a mathematic model that takes into account partial volume effects was used.^{3, 15} In this model, the CT number of each voxel, CT_i , is represented as a linear superposition of the signals from calcified and noncalcified tissues as follows: $CT_i = CT_{200} \times W_{CA} + CT_0 \times W_{NC}$ where CT_{200} denotes the CT number for a purely calcified voxel with a calcium density of 200 mg/ml, and CT_0 denotes the CT number for a purely noncalcified voxel with a calcium density of 0

mg/cc. W_{CA} and W_{NC} denote weights corresponding to the fractions of the voxel that contain purely calcified and noncalcified tissues, respectively. These weights satisfy the following relationship: $1 = W_{CA} + W_{NC}$. Solving for W_{CA} yields:

$$W_{CA} = \frac{CT_i - CT_0}{CT_{200} - CT_0}$$

The calcium density of the voxel, D_i , is simply

$$D_i = W_{CA} \times 200 \frac{\text{mg}}{\text{cc}} = \frac{CT_i - CT_0}{\left(\frac{CT_{200} - CT_0}{200 \frac{\text{mg}}{\text{cc}}} \right)} = \frac{CT_i - CT_0}{\text{Slope}}$$

This equation is illustrated in Fig. 9. CT_0 in the numerator of this equation was approximated by the mean CT number within the contralateral cylinder containing only normal saline. Since this reference CT number is computed from a region inside the phantom that is localized at the same depth from the surface of the phantom, beam hardening effects are thereby overcome.¹¹ If CT_0 was estimated directly from the standard bone mineral phantom, which was placed on top of the chest phantom, beam hardening effects would not be properly compensated. The expression in the denominator of this equation was approximated by the slope of the linear regression line fitted to the measured CT numbers in the 30-cm field of view and the known physical densities of the calcium hydroxyapatite in the standard bone mineral phantom.^{12, 13} Analysis has shown that this slope does not significantly change between independent scans performed during the same day.

To obtain the total calcium mass estimate for each arterial segment, the estimated calcium densities for each voxel were integrated over the cylindrical region corresponding to the arterial segment and then summed over all image slices that had evidence of calcium. This double summation is mathematically expressed as follows:

$$\text{Calcium mass} = \sum_{\text{slices}} \sum_i \frac{CT_i - CT_0}{\text{Slope}}$$

Because the CT numbers of soft tissues such as collagen, muscle, fat, and water are poorly differentiated, it was not possible to independently estimate plaque volume or mass from the EBCT data.